Comparative investigation of the surface properties of commercial titanium dental implants. Part I: chemical composition

C. MASSARO*, P. ROTOLO, F. DE RICCARDIS, E. MILELLA
PASTIS-CNRSM S.C.p.A, Biomaterials Unit, 7 Appia km 7 + 300, Brindisi, 72100 Italy

A. NAPOLI, M. WIELAND, M. TEXTOR, N. D. SPENCER
Laboratory for Surface Science and Technology, Department of Materials, Swiss Federal Institute of Technology, ETH-Zürich, CH-8092 Zürich, Switzerland

D. M. BRUNETTE
Faculty of Dentistry, University of British Columbia, Vancouver

The surfaces of five commercially available titanium implants (Brånemark Nobel Biocare, *3i* ICE, *3i* OSSEOTITE, ITI-TPS, and ITI-SLA) were compared by scanning electron microscopy, X-ray photoelectron spectroscopy, time-of-flight secondary ion mass spectroscopy. All five implant types were screw-shaped and fabricated from commercially pure (cp) titanium, but their surface properties differed both as regards surface morphology and surface chemical composition. The macro- and microstructure of the implant surfaces were investigated by scanning electron microscopy. The surfaces chemical composition was determined using the surface-sensitive analytical techniques of X-ray photoelectron spectroscopy and time-of-flight secondary ion spectrometry. Surface topographies were found to reflect the type of mechanical/chemical fabrication procedures applied by the manufacturers. The titanium oxide (passive) layer thickness was similar (5–6 nm) and typical for oxide films grown at or near room temperature. A variety of elements and chemical compounds not related to the metal composition were found on some implant types. They ranged from inorganic material such as sodium chloride to specific organic compounds believed to be due to contamination during fabrication or storage. The experimental findings are believed to make a contribution to a better understanding of the interplay between industrial fabrication procedure and physico-chemical implant surface properties.

1. Introduction

Titanium and its alloys are highly successful materials for the fabrication of dental and orthopedic implants, on account of their favorable combination of properties such as low specific weight, high strength to weight ratio, low modulus of elasticity, very high corrosion resistance and excellent general biocompatibility. The surface properties of titanium are particularly relevant [1–3] as the first contact of the body with the artificial material is through the surface. In particular, titanium implants are known to interact with bone tissue so that a large percentage of the implant surface will finally be in close contact with the newly formed bone tissue [4, 5], an observation that is important for the long-term stability and success of permanent implants.

The excellent biocompatibility and osseointegration capability of titanium is related to a variety of favorable properties of the material and its surface:

- A dense, highly resistant passive oxide film that protects the underlying metal from (further) oxidation and corrosion [3].
- A low dissolution rate of the oxide film and an extremely low concentration of charged titanium corrosion products [6]. The thickness and stability of the oxide film are relevant to implant performance as corrosion and ion release into the adjacent tissue [7] are undesirable.
- An acceptable biological response across the whole spectrum of interactions (water–proteins–cells), depending on the chemical and topographic properties of the surface [8, 9].
- A pronounced ability for osseointegration resulting in a high percentage of direct bone contact when directly implanted without the use of cement [10–13].

*Author to whom all correspondence should be addressed.

The composition of an implant surface can differ markedly from the bulk composition due to specific effects related to the manufacturing conditions, such as machining, thermal treatment, blasting, etching, coatings and sterilization procedures. Surface treatments generally leave traces of foreign material at the surface as a ''signature'' that is typical for the chosen type of treatment, such as metals or metal ions, lubricants, detergents or other specific chemical compounds. Such trace compounds may alter the surface properties even when present in very small quantities compared to the total (bulk) volume of the sample or device [14–16]. The presence of trace compounds or adventitious contaminants at the surface of the implant may also affect the response to the body after implantation and the formation of new tissue at the implant/body interface. There is relatively little known about the effects caused by specific contaminants at low concentration. In a study on titanium dental root implants retrieved from patients due to lack of osseointegration, specific elements (Pb, Zn, Sn) not normally present at a titanium implant surface were observed by surface analysis and discussed in the context of the observed failure of the devices to osseointegrate [17]. In view of these considerations there is widespread agreement that the careful control of implant surfaces and the measures taken to eliminate unwanted surface chemicals are important elements of quality assessment schemes. Compared to the long-standing tradition in monitoring bulk implant properties such as chemical composition (analysis), microstructure or mechanical properties, the systematic control of surface quality would appear to be relatively new and less established probably because specific sophisticated instrumentation and expertise are required to determine surface composition of thin films and of monomolecular or sub-monomolecular layers [18].

In the present work five different commercially available titanium (cp Ti) implants, produced by three major manufacturers (Nobel Biocare AB, *3i* Implant Innovation Inc., Institut Straumann AG) have been investigated in terms of surface morphology and composition. Currently dental implants are fabricated in a wide variety of designs, geometries and surface textures. We have selected and compared screw-shaped implants. The five implants show a wide variation in surface texture or morphology that must be the result of specific, proprietary fabrication and surface treatment protocols.

The aim of the present investigation is to describe and compare the surfaces of commercially purchased implant specimens including the thickness and chemical composition of the oxide layer. We used scanning electron microscopy (SEM) to image the surface macro- and microstructure and X-ray photoelectron spectroscopy (XPS) and time-of-flight secondary ion mass spectrometry (ToF-SIMS) to analyze the surfaces for their major and minor constituents as well as for inorganic and organic residues believed to be contaminants. All investigations were performed in the root part of the implant, which would contact bone *in vivo*.

In a subsequent paper, we will quantitatively describe and compare using several complementary techniques the surface topographies (''roughness'') on the same series of implants.

2. Materials and methods

2.1. Materials

Five types of endosseous, screw-type titanium dental implants with different surface finish were selected from three major manufacturers. All implants are based on commercially pure (cp) titanium. For each type of implant two specimens were purchased on the market. The implants were all received in their original sterile packaging and only opened at the start of the investigation. They were very carefully handled in order to prevent contamination during further manipulations. The type of implants, the corresponding manufacturers and the type of surface according to the manufacturer's information are listed in Table I. A photograph of the five types of dental implant studied is shown in Fig. 1.

2.2. Methods of surface characterization

Implants were analyzed as received without any preparation procedure. The analysis was always performed on the part of the implant surface intended for contact with bone.

2.2.1. Scanning electron microscopy

Scanning electron microscopy examinations were performed with a Philips XL40 LaB6 instrument equipped with an energy-dispersive spectrometer (EDS) EDAX DX4i. The beam acceleration voltage was 15 kV. Magnification ranged from 10–10 000 × . In order to judge local compositional differences across the surface,

TABLE I Investigated cp titanium solid screw implants

Type of implant	Abbreviation[1]	Type of surface[2]	Manufacturer
Brånemark® Implant System	Brånemark	Machined	NobelBiocare AB S-402 26 Göteborg Sweden
ITI® TPS	TPS	Plasma sprayed titanium	Institut Straumann AG CH-4437 Waldenburg Switzerland
ITI® SLA	SLA	Blasted and etched (duplex structure)	Straumann Ltd CH-4437 Waldenburg Switzerland
3i ICE®	ICE	Machined	*3i* (Implant Innovation Inc.), Palm Beach Gardens, FL 33410, USA
3i Osseotite®	Osseotite	Special microtexture	*3i* (Implant Innovation Inc.), Palm Beach Gardens, FL 33410, USA

[1] Short name used in the following text of this paper.
[2] According to information given by the manufacturer.

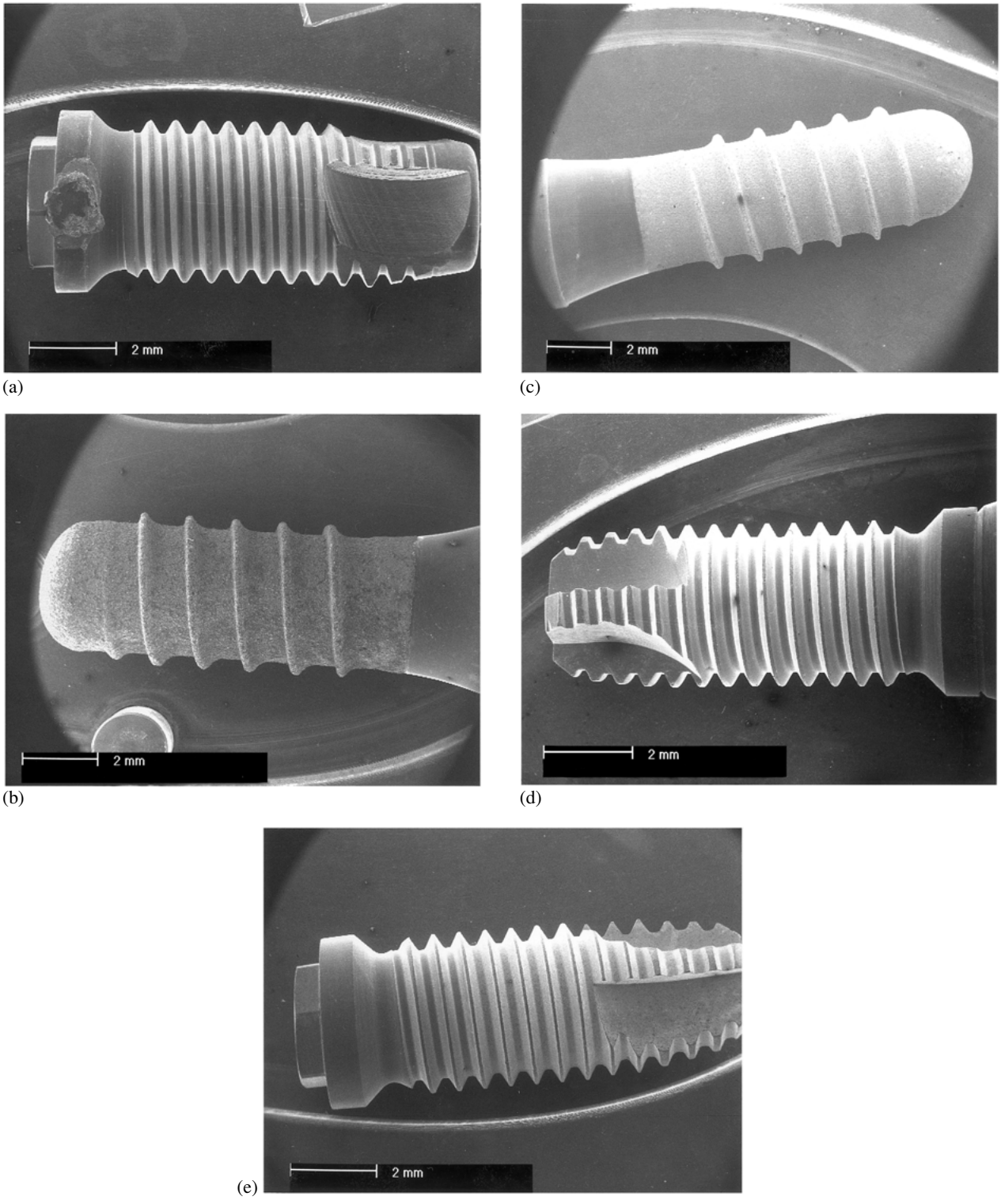

Figure 1 Photographs of the five types of implants used in this study (for details, see Table 1): (a) Brånemark implant; (b) TPS implant; (c) SLA implant; (d) ICE implant; (e) Osseotite implant (original magnification 7 × for all images).

observations were also made in the backscattered electron mode (BSE), complemented by local analysis using EDS and a finely focussed electron beam of 50 nm diameter.

2.2.2. X-ray photoelectron spectroscopy

X-ray photoelectron spectroscopy measurements were performed on a VG Scientific ESCALAB 210 electron spectrometer, operated with non-monochromatic AlKα radiation at a backpressure of $\sim 5 \times 10^{-9}$ mbar. The X-ray gun was operated at 15 kV and 300 W. Electron take-off angle (detection angle) was 90° for all measurements. The energy scale of the XPS instrument was calibrated by measuring the reference peaks Ag3d5/2 (BE = 368.26) on a clean silver foil and Cu2p3/2 (BE = 932.54) on a clean copper foil. All investigations were performed in the large area scan mode (5 × 5 mm) in order to improve the signal-to-noise ration. The sample holder was covered with a clean aluminum foil.

Survey spectra were recorded with a pass energy of 50 eV, detail spectra at high-energy resolution at 20 eV. All spectra were corrected for eventual sample charging by referencing the binding energies to the internal

standard of Ti2p3/2 of the TiO_2 layer at 458.8 eV, except for the implant ICE, where the Ti signal turned out to be too weak to be used as a reference. In the latter case the Si2p binding energy was set at 101.8 eV, typical for polydimethylsiloxane (PDMS), found to be the main surface component of this implant (see Results section).

The XPS data were quantified based on peak intensities after background subtraction (Shirley routine) and experimental sensitivity factors published by Wagner [19].

2.2.3. Time-of-flight secondary ion mass spectrometry

Secondary ion mass spectra of the as received dental implant surfaces were recorded on a PHI 7200 time-of-flight secondary ion mass spectrometer in the mass range 0–500 m/e. The total ion dose of the 8 kV Cs^+ primary ion beam ($100 \times 100\,\mu m^2$) was typically $1 \cdot 10^{12}$ ions $\cdot$ cm^{-2}, corresponding to a value below the static limit. Time per data point was 0.625 ns. Mass resolution M/M in the positive mode was typically 4500 (mass 48). To calibrate the mass scale, a standard set of low ion masses was used (PHI software TOFPAK).

3. Results

3.1. Scanning electron microsocopy investigation

All implants were imaged at different magnifications (from 20 × to 5000 ×) to provide a view of both the macrostructure of the device as well as the microstructure of the surface. Micrographs of the five types of implants are shown through Figs 2–6 at magnifications that best illustrate the various surface morphology features of the individual implants. At low magnification, all implants show a well defined, screw-type shape and a rather homogeneous surface appearance. At the higher magnifications, pronounced differences in morphology and topography become apparent:

Brånemark: The surface was characterized by a clearly visible, well-defined unidirectional structure, likely to be the result of machining. In addition small cavities, at relatively low density, protrusions and torn metal particles, typical for machined metal surfaces were observed. For the sake of simplicity we will call these locally observed structures ''defects''; the use of the term ''defect'' does not imply, either here or in the following text, any statement about the quality and performance of these devices, but merely deviation from a uniform surface structure. In some cases ''foreign'' particles embedded in the surface region were found. EDS analysis showed these to be mainly composed of Na, S and Cl (Figs 2(a), (b)).

TPS: The surface was clearly much rougher than Brånemark implant and seemed to be almost completely covered by the thermally sprayed titanium layer. The micro-structure is typical for plasma sprayed metal coatings with individual molten metal droplets that have arrived at the surface with high speed and have solidified in contact with the (titanium) substrate. There was a high proportion of ''open-porous'' structure

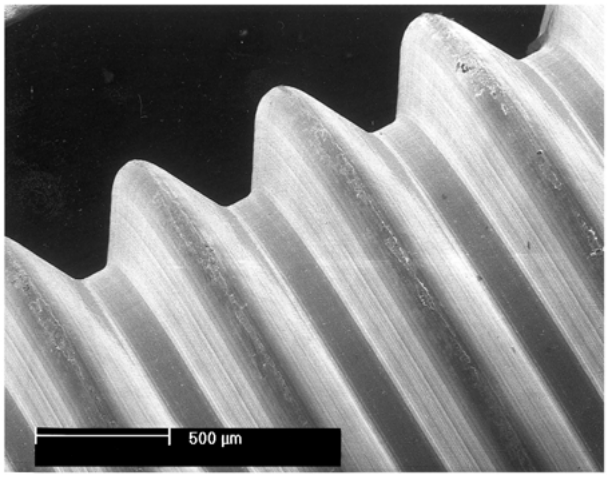

(a)

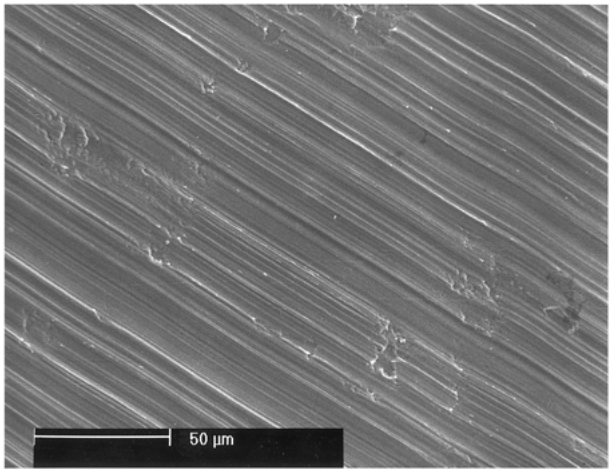

(b)

Figure 2 SEM micrographs of the implant type Brånemark: (a) original magnification 50 × ; (b) original magnification 500 × .

visible, typical for coatings that have been plasma sprayed in air. (Fig. 3(a)–(c)).

SLA: A duplex surface morphology was clearly evident for this type of titanium surface with indentations or cavities of the order of roughly 20–50 µm diameter. A much finer microstructure with cavities of typically 0.5 to a few µm diameter was superimposed onto the rougher structure. According to information given by the manufacturer this duplex structure is achieved through a combination of a blasting operation (coarse structure) followed by a chemical etching procedure (fine structure). In a very few instances, particles of several tens of micrometers embedded into the surface were detected. Local analysis showed a predominant aluminum signal. These particles are likely to be alumina residues from the blasting process (Fig. 4(a)–(c)).

ICE: This surface also showed a microstructure typical for machined parts. Again, as in case of the ''Brånemark'' implant, local ''defects'' (in the sense defined above) typical for machined surfaces were evident. Based on the surface areas investigated, the density of these local ''defects'' appeared to be higher on this surface compared to the ''Brånemark'' type, but no quantitative comparison was undertaken (Fig. 5(a)–(b)).

Osseotite: A surface texture different from all others is evident on this implant type, characterized by a ''crystallographic'' appearance and a very fine cavity-

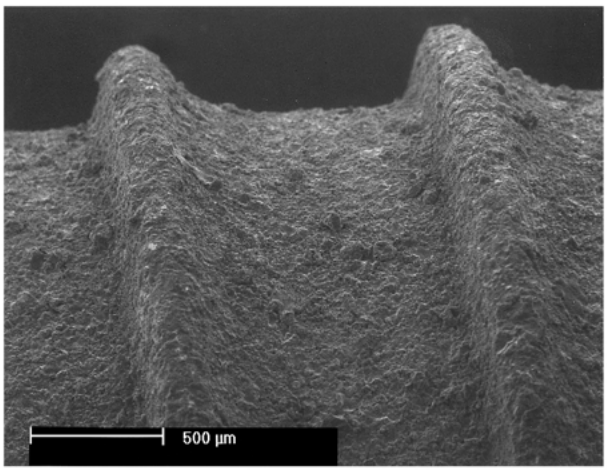

(a)

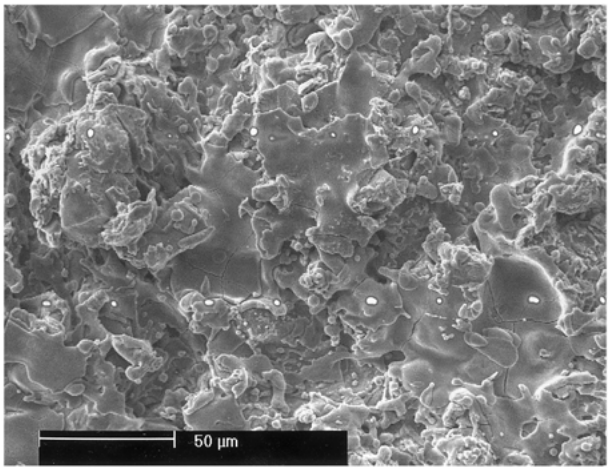

(b)

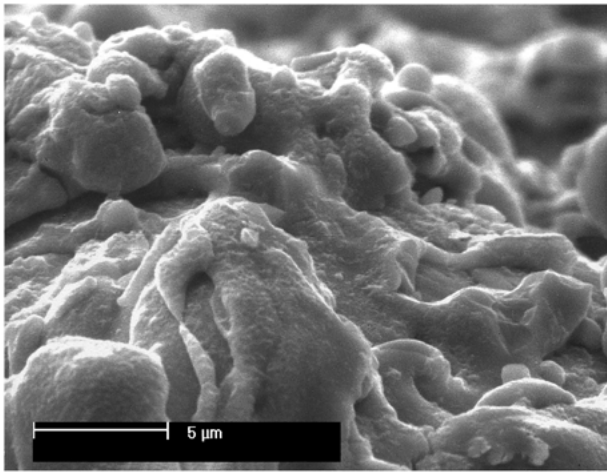

(c)

Figure 3 SEM micrographs of the implant type TPS: (a) original magnification 50 × ; (b) original magnification 500 × ; (c) original magnification 5000 × .

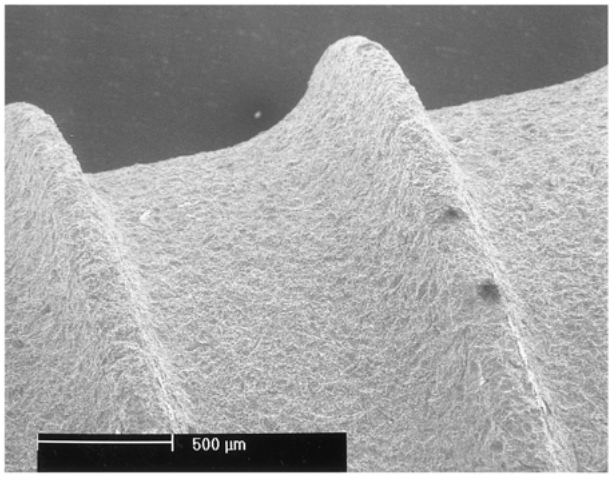

(a)

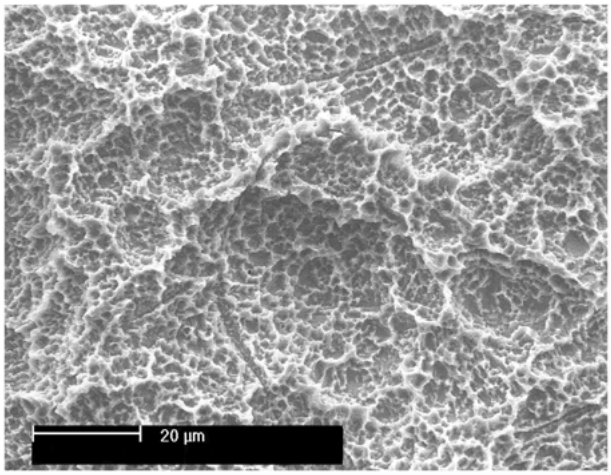

(b)

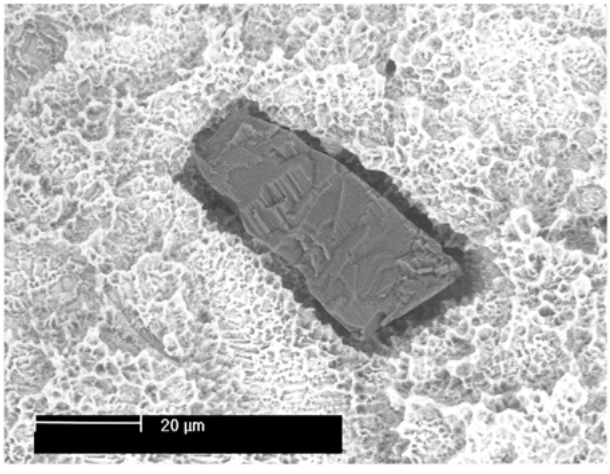

(c)

Figure 4 SEM micrographs of the implant type SLA: (a) original magnification 50 × ; (b) original magnification 1000 × ; (c) original magnification 1000 × .

like microstructure with dimensions well below the micron range. The surface gave the impression of a crystallographically etched structure that arises when local dissolution rates depend on the orientation of individual titanium metal grains. The morphology of the fine structure also depends on the orientation of individual grains. In addition, at medium to high magnification one could often find local areas where the etch structure differed due to local inclusions in the metal surface. At such sites electrochemically steered local dissolution with adjacent cathodic and anodic sites can occur. EDS analysis indicated these inclusions to be composed of Fe and A1. At high magnification there was clear indication for preferred dissolution of titanium at grain boundaries as there were narrow gaps between adjacent grains. In BSE mode, composition contrast was evident with small ''spots'' composed of lighter material than the rest of the surface, and therefore appeared dark in the electron micrograph. Local analysis by EDS showed these ''spots'' to be composed of sodium, silicon,

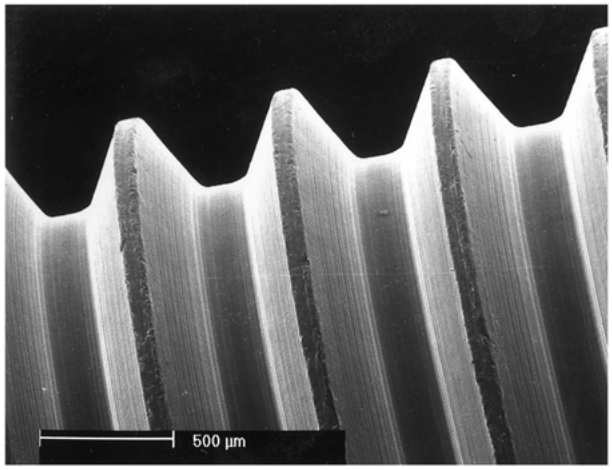

(a)

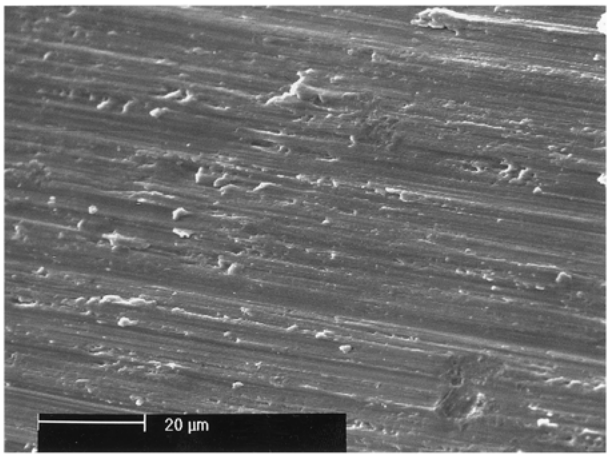

(b)

Figure 5 SEM micrographs of the implant type ICE: (a) original magnification 50 × ; (b) original magnification 1000 × .

potassium and sulphur. The density of these contaminants was highest at the top of the threads (Fig. 6(a)–(d)).

3.2. X-ray photoelectron spectroscopy

In Figs 7 and 8 the XPS survey spectra of two implant surfaces are presented. These two spectra give an impression of the range of differences observed for the different surfaces investigated in this study. The survey spectra of the other three implants are not given, as the relevant information is summarized in a quantitative manner for all implants in Tables II–IV. As there was close agreement between the spectra of the duplicate implant samples, we may therefore conclude that the results are typical for the corresponding implant type and fabrication batch. Table II lists the quantitative results of the elements detected with sufficient intensities to allow quantification. An element was considered to be present at the surface, if the corresponding signal-to-noise ratio in the high-resolution detail spectrum was at least 3. The quantitative results should be interpreted with caution, as the different types of surfaces differ highly in terms of surface roughness. For rougher surfaces such as for TPS or SLA, the concentrations of surface contaminants (mainly adventitious hydrocarbon) would be expected to be overestimated to some extent as a result of local angular effects.

3.2.1. Titanium

The Ti2p1/2 and Ti2p3/2 high-resolution spectra were all deconvoluted into three sub-peaks following a procedure described previously [20, 21]. The full width at half-maximum height was fixed at the following values: 2.2 eV for the Ti2p1/2 subpeaks and 1.6 eV for Ti2p3/2 subpeaks. The peak components of Ti2p1/2 and Ti2p3/2 labeled A, B, C and D, E, F respectively can be attributed to titanium in the oxidation states IV (TiO_2), III and II (Ti_2O_3 and TiO) and 0 (Ti metal). On account of the low intensities and close positions of Ti III and II, these two components have been treated as one sub-peak in the curve fitting. As expected [21], the peaks corresponding to TiO_2 are by far the most prominent ones in the Ti2p region. As a representative example, the deconvoluted Ti2p spectrum of implant Brånemark is shown in Fig. 9. The binding energies of the components are shown in Table III.

Titanium oxide layer thickness has been calculated based on the experimental peak area ratio of Ti2p3/2(oxide)/Ti2p3/2(metal). The calculation involves standard equations [23] and quantitative values for the densities of Ti and TiO_2 as well as for the mean free path of Ti2p electrons in the metal and oxide respectively [21, 22]. The titanium oxide layer (passive film) was found to be in the range of 5.4–5.7 nm across the implants investigated. The composition of the oxide film in terms of the components assigned to Ti(IV), Ti(III, II) and Ti(0, metal) were quite similar as shown by the relative peak areas of the components in Table IV. It

TABLE II Surface elemental composition and titanium oxide layer thickness of the five dental implants investigated, calculated from XPS intensities

Implant type	Surface concentration [atom%][1]								Oxide layer thickness [nm]
	Ti	O	C	Si	Na	F	Cl	N	
Brånemark	12.8	51.9	29.8	—	5.0	—	0.5	—	5.7
TPS	14.2	45.5	38.9	—	Traces[2]	Traces[2]	—	1.4	5.5
SLA	14.5	51.4	34.9	Traces[2]	—	—	—	1.3	5.7
ICE	0.9	21.1	71.9	6.1	—	—	—	—	n.d.[3]
Osseotite	6.8	36.2	53.7	3.3	Traces[2]	—	Traces[2]	5.4	

[1]The given values should be considered with an error of approx. ± 15% relative.
[2]Traces: these elements have been detected at a signal-to-noise ratio > 3, but the intensity is too low for quantification.
[3]No determination possible as the titanium oxide layer was hidden by a top surface layer composed mainly of C, Si and O (see text).

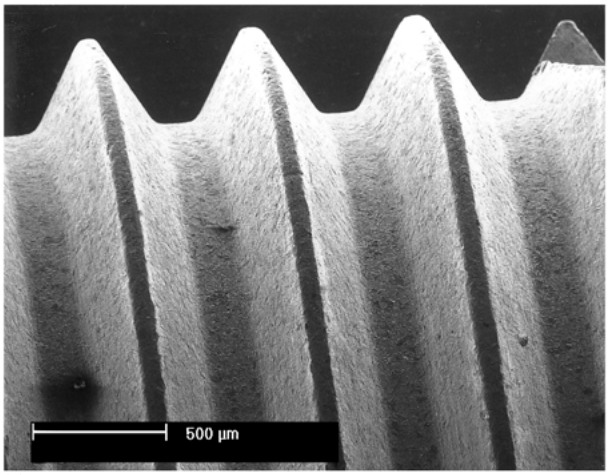

(a)

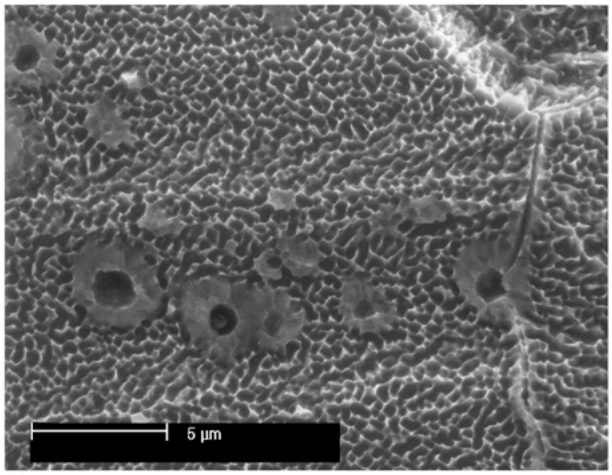

(c)

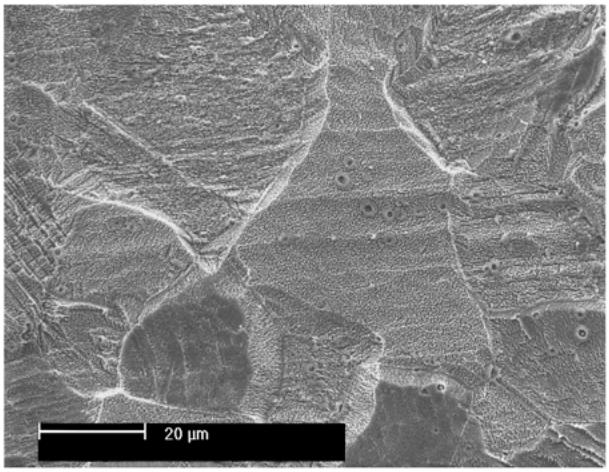

(b)

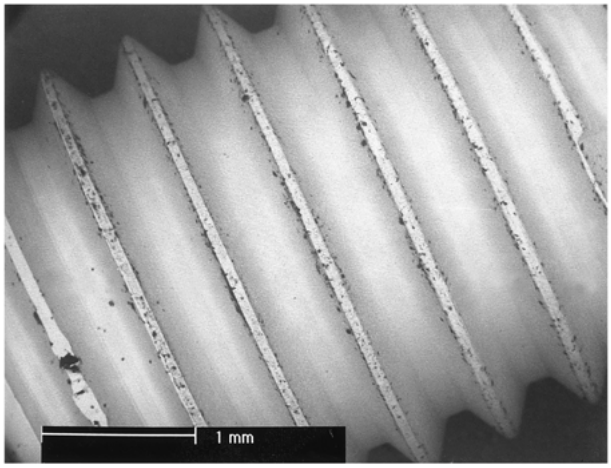

(d)

Figure 6 SEM micrographs of the implant type Osseotite: (a) original magnification 50 × ; (b) original magnification 1000 × ; (c) original magnification 5000 × ; (d) BSE mode, original magnification 28 × .

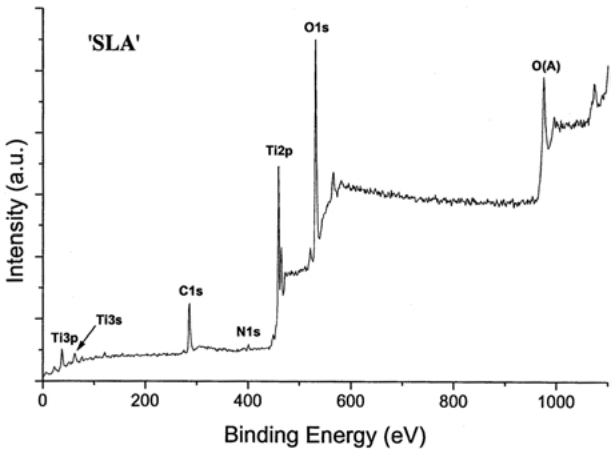

Figure 7 XPS survey spectrum of implant SLA.

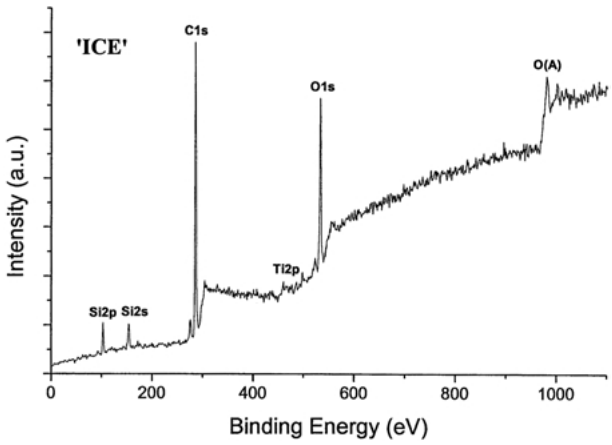

Figure 8 XPS survey spectrum of implant ICE.

should, however, be mentioned that that the determination of oxide film thickness also depends on surface roughness. The complexity of the topography on some of the implants means that the thickness of the oxide layer cannot be estimated strictly quantitatively. We should therefore state that the reproducibility of the oxide thickness determination is excellent (typically $\pm$ 0.1 nm), but the absolute value may show somewhat larger variations between the different implant types than one deduces from Table II. On the other hand, the values found (5–6 nm) are very typical for the room temperature passive oxide layer thickness formed on cp titanium [21].

However in the case of Osseotite implant, the observed Ti2p intensities were very low and prevented any type of curve fitting into individual components

TABLE III Binding energies (± 0.1 eV) of the deconvoluted XPS detail spectra in the Ti2p, O1s and C1s region and assignment to chemical species

Implant	XPS binding energies [eV]								
	Ti2p			C1s			O1s		
	TiO_2	Ti_2O_3 + TiO	Ti (met.)	C–C C–H	C–O	COO or C=O	Type A (TiO_2)	Type B (see text)	Type C (see text)
Brånemark	458.8[1]	456.0	454.0	285.0	285.9	289.0	530.3	532.2	533.7
TPS	458.8[1]	456.3	454.3	285.0	286.1	287.7	530.3	532.2	533.9
SLA	458.8[1]	456.3	454.3	285.0	286.3	288.4	530.4	532.2	533.7
ICE	458.3[2,3]	—	—	284.5[2]	286.1	288.6	529.5	532.0[2]	—
Osseotite	458.8[1]	456.1	454.0	285.0	286.2	289.0	530.3	532.3	533.7

[1]Set to 458.8 eV as internal energy scale reference.
[2]Internal calibration: Si2p set to 101.8 eV (see text).
[3]Error of approx. ± 0.4 eV due to low signal intensity.

TABLE IV Results of the deconvolution of the XPS Ti2p, C1s and O1s spectra: relative areas of peak components

Implant	Relative proportion (peak area) [%]								
	Ti2p			C1s			O1s		
	TiO_2	Ti_2O_3+ TiO	Ti (met.)	C–C C–H	C–O	COO or C=O	TiO_2	Type B (see text)	Type C (see text)
Brånemark	88.2	5.5	6.3	30.0	59.3	10.7	48.9	36.4	14.7
TPS	85.5	7.4	7.1	26.3	36.8	36.9	60.7	22.2	17.1
SLA	87.8	5.8	6.4	42.2	39.0	18.8	65.7	17.7	16.6
ICE	(100)[1]	—	—	81.1	14.5	4.4	15.3	84.7	—
Osseotite	86.3	6.1	7.6	47.7	43.0	9.3	37.7	34.0	28.3

[1]Due to very low intensity, no deconvolution of the Ti2p signal was feasible for implant ICE.

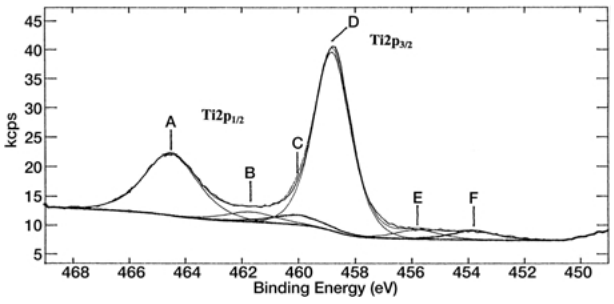

Figure 9 XPS Ti2p1/2 (A, B, C) and Ti2p3/2 (D, E, F) spectrum of implant Brånemark with deconvolution into oxide (A, B, D, E) and metal (C, F) components.

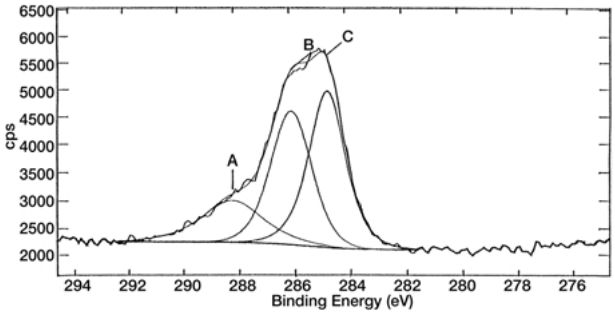

Figure 10 XPS C1s spectrum of implant SLA deconvoluted into three chemically different components.

because the titanium oxide film is covered by an additional layer composed of C, O and Si. This top layer must be on average several nanometers thick since the sampling depth of the XPS technique at the kinetic energy of the Ti2p electrons and 90° take-off angle is typically 7 nm. The chemical nature of this layer is further discussed below.

3.2.2. Carbon

The Cls signals were curve-fitted based on three different components. Fig. 10 shows a representative spectrum for implant SLA. The deconvolution is straightforward as well as the assignment to hydrocarbon (285.0 eV), C–O species (ca. 286 eV) and COO species (288–289 eV) (Table III). The presence of carbon in different chemical environments is typical for titanium (and other metal) oxide surfaces. This is a consequence of the tendency of titanium surfaces to readily adsorb organic components during fabrication (e.g. lubricants) or during storage from the ambient atmosphere. The relative peak areas are listed in Table IV, while Fig. 11 shows the C1s spectra for all implant types investigated. There were differences in the relative proportion of the individual peak components.

3.2.3. Oxygen

Following procedures established in the literature [21, 22], the O1s signal was curve-fitted based on three individual components. An example is given in Fig. 12 (implant SLA), while Fig. 13 shows all O1s spectra for comparison. The assignment of binding energy 530.3 eV to TiO_2 is straightforward [23]. For relatively clean

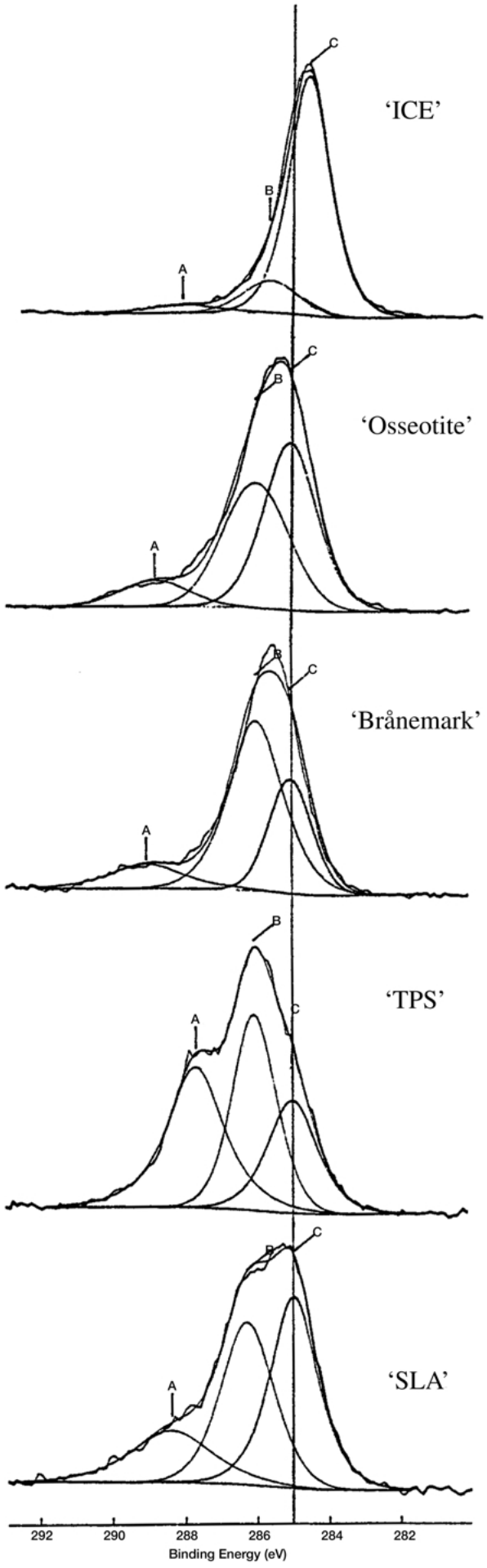

Figure 11 XPS C1s spectrra of all implant surfaces investigated.

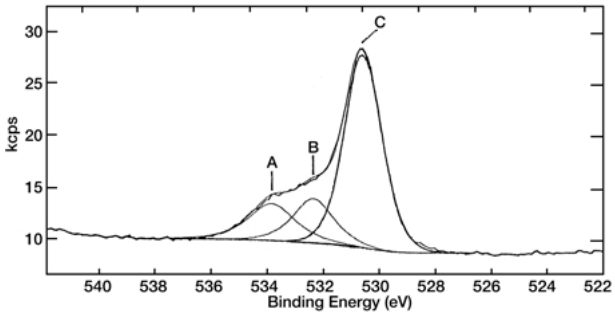

Figure 12 XPS O1s spectrum of implant SLA deconvoluted into three chemically different components.

titanium surfaces, this peak always dominates the O1s region [21], as was true for the implants TPS, SLA and Brånemark (Table IV, Fig. 13). The O/Ti atomic ratio calculated from the peak areas of O1s (530.3 eV) and Ti2p3/2 (458.8 eV) were found to be 2.2 ± 0.2, 2.2 ± 0.2 and 2.6 ± 0.2 for the three implants Brånemark, TPS and SLA respectively. This is close or slightly higher than the ratio of 2 : 1 expected for a perfect TiO_2 stoichiometry. The slight deviation may be due to some additional oxygen present at the surface or within the oxide film with oxygen binding energies close to the one of TiO_2.

The components at ca. 532 eV (called type B in Table III and IV) and ca. 533–534 eV (type C) were more difficult to assign. Hydroxides (–OH) and adsorbed water (H_2O) are believed to give rise to emissions around those two binding energies. In addition however, oxygen bound in organic compounds (e.g. C═O and C–O) can also demonstrate binding energies in this energy range. As the C1s region shows substantial presence of carbon bound to oxygen, at least part of the higher energy emissions in the O1s spectra have to be attributed to organic, O-containing molecules that are either adsorbed to or have reacted (i.e. covalently bound species) with the titanium oxide surface. This is particularly true for the implant Brånemark which showed both a high proportion of the C1s signal at ca. 286 eV (C–O) and of the O1s signal at ca. 532 eV. Similarly implant TPS showed high C1semission intensity at around 288 eV (COO) paralleled by a relatively strong O1s contribution in the range 532–534 eV.

Again, the implants ICE and Osseotite were found to have a surface chemistry substantially different from all others. Here the main O1s peak was situated at a binding energy of ca. 532 eV, while the TiO_2 related peak at 530.3 was relatively weak, particularly for ICE, when compared to the other implant surfaces. The conclusion is that for both, but in particular for implant ICE, the passive oxide film was covered by an additional layer that was composed of C, O, and Si.

3.2.4. Other elements

Few additional elements were detected by XPS in small or trace concentrations. The high silicon (Si) content of the ICE and – to a lesser extent – of the Osseotite surface was unexpected. The Si2p binding energy of 101.8 eV would be consistent with the presence of an organosilicon compound. It is, however, not possible from XPS to draw definitive conclusions as regards the type or origin of this chemical species.

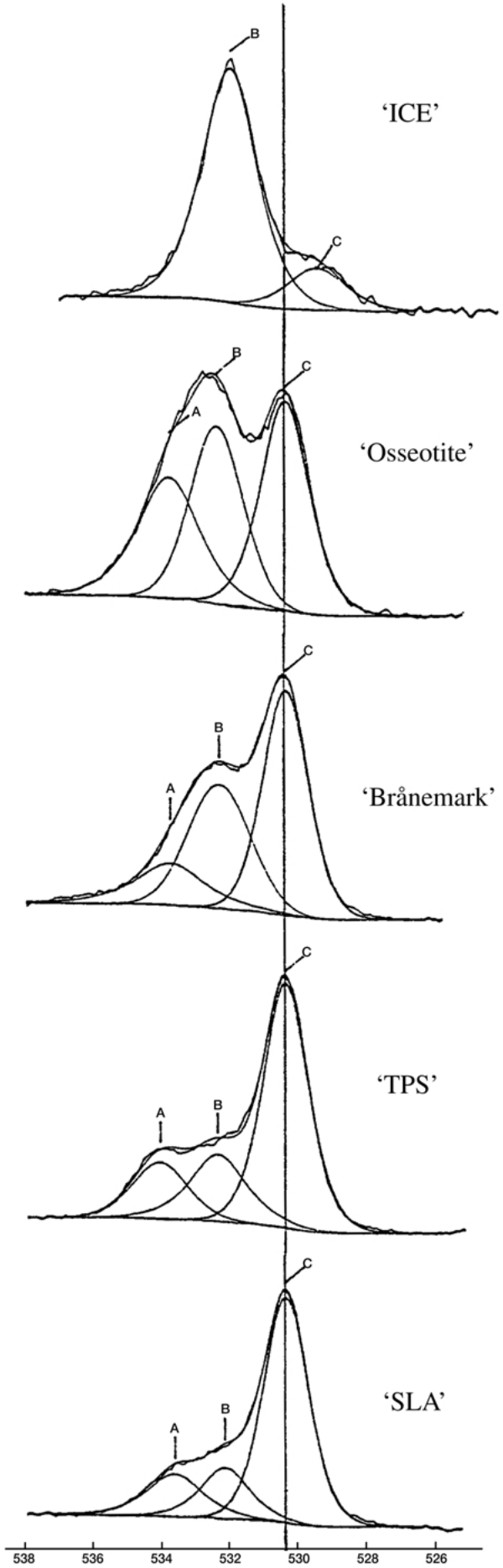

Figure 13 XPS O1s spectra of all implant surfaces investigated.

Also significant was the relatively high sodium (Na^+) concentration, accompanied by a much smaller chloride (Cl^-) content on the surface of the Brånemark implant. As the sodium concentration greatly exceeded the chloride concentration, it is obvious that the sodium content cannot be exclusively due to deposition of NaCl, but must be partly linked to other anions in the surface or alternatively be incorporated in the titanium oxide film. Nitrogen was detected at low concentration on TPS and SLA implants. The low binding energy of 396.9 eV detected for the N1s signals on the TPS implant suggest that the nitrogen is present as titanium nitride on this implant. Small amounts of titanium nitride are expected for titanium layers plasma sprayed in air, as the titanium metal droplets either react with oxygen (to form oxides) or nitrogen (to form nitrides). An additional N1s signal was detected at 401.1 eV on the SLA implant suggesting the presence of small amounts of organic nitrogen-containing species or of ammonium, a rather common contaminant on surfaces of industrial products.

3.3. Time-of-flight secondary mass spectrometry

There are three reasons why we used ToF-SIMS for surface analysis in addition to XPS: first ToF-SIMS is more surface-sensitive than XPS as it probes only the outermost few atomic or molecular layers. The information therefore stems from that part of the surface layer that is believed to be decisive to biologically relevant processes in the very early stages of implantation, such as

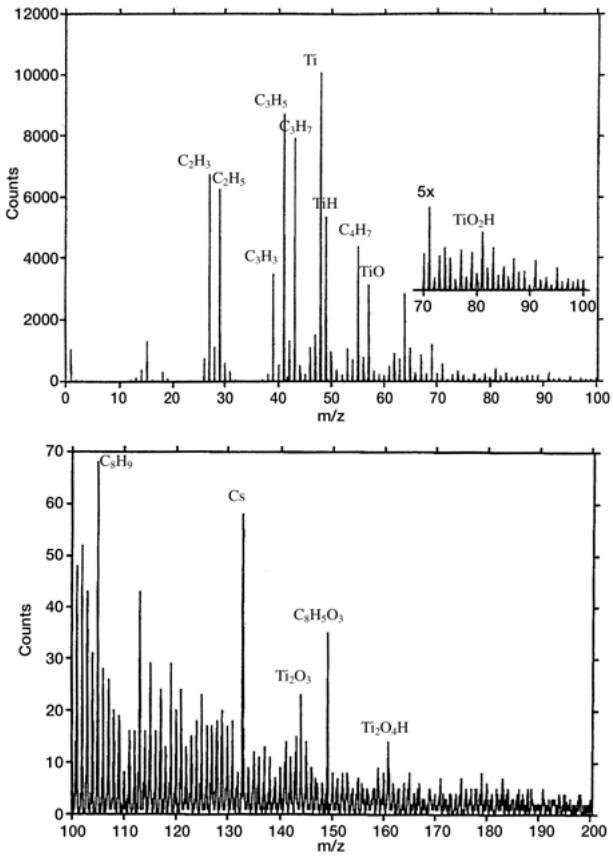

Figure 14 ToF-SIMS spectrum (positive secondary ions) of implant SLA in the mass range 0–200 m/z.

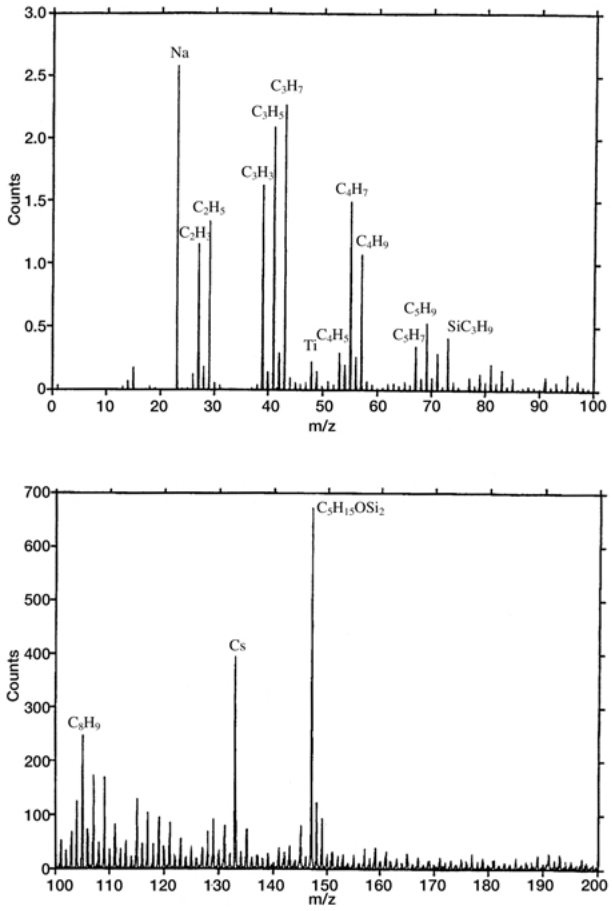

Figure 15 ToF-SIMS spectrum (positive secondary ions) of implant ICE in the mass range 0–200 m/z.

adsorption of proteins, glycoproteins, lipids and carbohydrates. Secondly, SIMS has the advantage of very high detection sensitivity. This can help to get more reliable information on trace concentrations of compounds at the surface that may be undetectable or hardly detectable by XPS. Thirdly, in contrast to XPS with chemical information restricted to nearest and next-nearest neighbors, ToF-SIMS has the potential to disclose molecular information, particularly about organic molecules at the surface; it is therefore complementary to XPS. The main disadvantage is that secondary ion emission is strongly dependent on the chemical matrix. Hence there is no straightforward way to turn count rates into surface concentration and analyses are generally considered to be qualitative. Since we are dealing with similar matrices in this study, however, one may consider relative intensities of particular types of emitted secondary ions to reflect changes in surface concentrations in a semi-quantitative way [18].

Again as in XPS, we just present ToF-SIMS spectra in two cases in order to illustrate the range of differences in secondary ion intensities for two ''extreme'' cases: SLA (Fig. 14) and ICE (Fig. 15). Fig. 14 shows a spectrum that is typical for a titanium (oxide) surface with a relatively low amount of organic compounds at the surface (mostly unavoidable, adventitious hydrocarbon contaminants). Ions originating from the titanium oxide film surface such as Ti^+, TiO^+, TiO_2H^+, $Ti_2O_3H^+$, $Ti_2O_4H^+$, are clearly apparent in the spectrum with appreciable intensities. Fragmentation of the organic adlayer leads to secondary ions of the type $C_aH_b^+$, $C_aH_bO_c^+$. In the spectrum of the ICE implant (Fig. 15) on the other hand, ion intensities related to the titanium oxide layer are much weaker implying that only a relatively small fraction of the outermost surface is composed of titanium oxide. In addition to species of the type $C_aH_b^+$, $C_aH_bO_c^+$, also observed for the other implants, additional peaks due to organosilicon compounds are clearly detected in Fig. 15 (m/e = 73 and 147). These fragment ions are characteristic of polydimethylsiloxane (PDMS) [24], a highly surface-active contaminant often found on surfaces. It can, therefore, be concluded that the high silicon intensities found by XPS on implant ICE was not due to inorganic silicon oxide or silicates, but due to PDMS. Moreover, inorganic species, in particular Na^+, that have very high detection sensitivity down to the ppm range, are detected as well.

In order to be able to compare relative intensities in a semi-quantitative manner, the intensities of classes of fragment patterns have been determined. They are presented in Table V both as percentage of the sum of all intensities registered as well as ratioed relative to the sum of titanium oxide related secondary ion intensities. Such ratios are very sensitive functions of the 'cleanliness' of a surface, but should only be considered as semi-quantitative indicators.

Comparing the ToF-SIMS data and the quantitative XPS results one finds a general correlation that seems reasonable in view of the semiquantitative nature of the SIMS information:

- The sum of the carbon-containing secondary ion intensities relative to those related to the titanium oxide film are highest for ICE and Osseotite; in agreement with the XPS findings.
- There are two surfaces that exhibit silicon-containing secondary fragments: particularly ICE and – to a lesser extent – Osseotite. The masses observed at m/z = 73 and 147 have clearly been identified as $Si_3H_9^+$ and $C_5H_{15}OSi_2^+$ respectively. These are typical fragments of polydimethylsiloxane (PDMS)[24] as noted above. Since these two surfaces show substantial amounts of silicon in

TABLE V Relative ToF-SIMS intensities (positive ion mode) of classes of ion fragments

Class of fragments	Relative secondary ions intensities (%)[1,2]				
	Brånemark	TPS	SLA	ICE	Osseotite
$\sum(Ti + Ti_aO_b)$	7.9[1]	33[1]	27[1]	3.5[1]	14[1]
	1.0[2]	1.0[2]	1.0[2]	1.0[2]	1.0[2]
$\sum(C_aH_b)$	32	51	70	78	77
	4.0	1.5	2.6	22	5.5
$\sum(Si_aC_bO_cH_d)$	—	—	—	5.9	2.0
	—	—	—	1.7	0.1
$\sum(C_aO_bH_c)$	1.2	3.6	2.8	5.4	3.7
	0.2	0.1	0.1	1.5	0.3
$\sum(C_aO_bN_cH_d)$		7.2	0.5		2.9
	—	0.2	0.02	—	0.2
Na	59	5.2		7.7	0.4
	7.5	0.2	—	2.2	0.03

[1]Sum of intensities of indicated fragment types relative to the sum of intensities of all peaks observed and assigned.
[2]Sum of intensities of indicated fragment types relative to the sum of titanium oxide related secondary ions.

XPS, it is highly likely that the source of silicon is in fact PDMS.

- $^{23}Na^+$ had the highest relative intensity for the implant surface Brånemark, in agreement with the XPS finding. Smaller relative intensities of $^{23}Na^+$ were found for some of the implants, as was the case in XPS.

4. Discussion

Five commercial cp titanium implants with different surface properties produced by three manufacturers have been analyzed using SEM, XPS and ToF-SIMS. It should be made clear that the techniques used in this study are only probing the surfaces (topography/morphology, chemical composition), no information is given on important properties that are more closely related to the bulk composition and microstructure. More specifically, XPS is a technique with a sampling depth of approximately 7 nm for titanium surfaces, while ToF-SIMS is even more surface-sensitive actually probing only the outermost few atomic or molecular layers. The techniques are complementary in the sense that XPS has an ideal sampling depth for studying titanium oxide passive films believed to be essential for both the corrosion resistance as well as for biocompatibility aspects of titanium implants [6]. ToF-SIMS on the other hand essentially probes the degree and nature of surface contaminants with very high detection sensitivity; this information is however qualitative or at best semiquantitative. Another limitation is the fact that one has to be careful when comparing either XPS or SIMS results from surfaces that substantially differ in terms of surface topography and roughness.

A second general remark relates to the fact that only two specimens were investigated per type of implant. With such limited sample no conclusions can be drawn with regard to the degree to which these samples are typical of the manufacturer's production, neither within the particular batch nor between batch. This would require a large-scale study outside the scope of the current investigation. On the other hand, the experimental findings and the differences between the various types of surfaces turned to be characteristic for different areas of the same device as well as between the two specimens investigated per implant type.

With these limitations in mind, the following conclusions result from this study:

1. The surfaces of implants Brånemark, TPS, SLA and Osseotite, for which a strong XPS titanium signal is recorded, show a well-defined titanium oxide layer (passive film) mainly composed of titanium dioxide (TiO_2). The thickness of this oxide film is estimated to be 5.5–5.7 nm, a range that is typical for natural oxide films grown at or around room temperature. For implant ICE the XPS titanium-related signals had too low an intensity to allow peak deconvolution which is needed to calculate the oxide film thickness. The reason is that the oxide film in this particular case is 'hidden' by a top surface layer of organic nature. We do not imply that there is no well-defined oxide film on this surface. It is very likely that the contrary is true, but the organic overlayer on this particular implant surface must have a thickness comparable to the sampling depth, thus preventing detailed analysis by such surface-sensitive techniques. We deliberately did not sputter (i.e. removing surface contamination by ion etching), since it is well known that the surface chemistry (stoichiometry) is altered by ion bombardment. Also rough surfaces are in general not well suited for quantitative depth profiling and show artefacts due to uneven removal of surface material.

2. As regards surface species other than titanium oxide, we observe major differences between the different types of implants. These additional species are of both inorganic and organic nature. Sodium is a frequently observed element on oxide surfaces. The highest relative intensities within this study were observed on the implant Brånemark, the lowest on SLA. The results suggest that Na^+ is only partly linked to chloride (NaCl), and may be related to salts of organic acids, e.g. carboxylates that were also indicated from the deconvoluted XPS C(1s) spectra. The origin of the organic acids could be residues from tensides used in the fabrication, e.g. during chemical cleaning stages. Another explanation for the high Na^+ signal could be that Na^+ ions are incorporated into the titanium oxide film. Also, rather small amounts of nitrogen-containing species were observed on surfaces TPS, SLA and Osseotite. In the first case, the nitrogen is clearly due to nitride (titanium nitride) as a consequence of the reaction of nitrogen with titanium droplets in the atmospheric plasma titanium spray process. For SLA and Osseotite on the other hand, nitrogen is more likely to be due to either organic species or ammonium residues.

3. Organic contamination was observed on all surfaces which is not surprising as every titanium (oxide) surface exposed to air will adsorb hydrocarbons or carbon–oxygen containing species from air. This is unavoidable in practice and happens as soon as (clean) titanium (as well as other metal) surfaces are exposed to ambient conditions. There were, however, differences between the implants investigated as regards the level of organic carbon at the surface: the highest level was clearly observed for implant ICE, while implants Brånemark, SLA and TPS showed comparatively low levels. The high level of carbon and silicon on implant ICE resulted from organic silicon residues, most likely polydimethylsiloxane (PDMS, see ToF-SIMS results). This is a highly surface-active chemical frequently observed on surfaces by highly surface-sensitive techniques. There are different ways in which siloxane contaminants could be introduced. Siloxane could be part of the formulation or a contaminant of the surface cleaning procedures used in the processing, or it could originate from residues of silicon lubricants used in fabrication.

Highly different surface topographies or morphologies were observed on the five different types of implant surfaces investigated in this work, that obviously reflected the different approaches taken by the three manufacturers to surface engineering of the bone-contacting portion of the dental implant. Surface microstructure or roughness is known to be important

for the material–cell and material–tissue interactions during the osseointegration process. Two of the five investigated implants (Brånemark, ICE) have surface morphologies that are obviously produced during machining, characterized by a relatively smooth surface and typical groove structure due to the machining (e.g. turning) operation. All three other surfaces were unique as regards their topography/morphology. Implant TPS shows a morphology typical of a thin, plasma sprayed titanium layer. This process induces a certain morphology related to the size, temperature and kinetic energy of the molten titanium particles impinging on the substrate (again titanium in this case). Simultaneously, a relatively high proportion of open surface porosity is formed in this process believed to be advantageous for cell–surface interactions and tissue ingrowth [10, 11] The implants SLA and Osseotite showed both fine structures characteristically produced by chemical etching processes. However, the two surfaces are clearly different, both as regards the dimensions of the surface microstructures as well as the homogeneity. On Osseotite implant there are local height differences related to the grain structure of the base metal, on which the very fine etch structure is superimposed. The etch structure dimensions do not seem to be homogeneous across the surface, but appear to locally depend on the crystallographic orientation of the metal grain. Also, preferential grain boundary attack was often observed. In the case of the implant SLA one observes a clear duplex structure: a coarser microstructure as a consequence of a particle blasting process. Obviously microcrystalline Al_2O_3 particles were used in the blasting process, since, in rare cases, individual alumina oxide crystals could be found embedded into the titanium surface. A finer etch-type structure (but somewhat coarser than in case of Osseotite) that is relatively constant in dimensions and fairly regularly distributed across the surface was superimposed on the coarser blasted structure. Preferential grain boundary attack could not be observed on this implant surface.

Although differences in surface properties and composition were found among the implants used in this study, it is not clear whether these differences actually alter the performance of the various implant systems *in vivo*. Indeed one could conceive of scenarios where particular surface contaminants might be advantageous, for example if they favored the deposition and appropriate conformation of proteins involved in cell adhesion. Nevertheless, contaminants have the potential to alter implant performance, and manufacturers should be aware of their presence if for no other reason than to deliver identical surfaces over time. Thus, quality control regimes should include inspection by detailed surface analysis techniques such as XPS and ToF-SIMS. As the different surface topographies and chemical compositions have the potential to alter implant performance, more detailed studies are required to delineate their specific effects on biological responses such as osseointegration. It should be emphasized that all of the implant systems examined here have been reported to demonstrate acceptable performance when implanted *in vivo*. But there may be differences between the systems that would be difficult to detect in clinical controlled trials which typically use relatively few implants of each type, and thus lack statistical power. Thus, detailed studies on the effects of topography and chemical contaminants might be most feasibly conducted in animal model systems where greater numbers of implants could be tested for their effects on biological responses under well controlled conditions in reasonable time.

In view of the importance of surface topography/morphology of implants for the osseointegration process, surface topography and roughness of the same implants studied in this work will be measured quantitatively using different contact and non-contact profilometry techniques. The comparative results will be evaluated and published separately as Part II of this investigation into the surface properties of commercial dental implants.

Acknowledgments

The authors thank the Italian Ministry of the University and the Scientific and Technologic Research (MURST) that supported this work in the frame of an innovation project on dental bioengineering.

References

1. J. LAUSMAA, *J. Electron Spectr. Rel. Phenom.* **81** (1996) 343.
2. D. C. SMITH, R. M. PILLAR and G. MURRAY, *Trans. 11th Annu. Meeting Soc. Biomater.* **8** (1985) 8.
3. B. KASEMO and J. LAUSMAA, *J. Biomed. Mater. Res.* **22** (1988) 145.
4. J. J. COLLIS and G. EMBERY, *Biomaterials* **13** (1992) 553.
5. C. B. JOHANSSON, H. A. HANSSON and T. ALBREKTSSON, *ibid.* **11** (1990) 277.
6. S. G. STEINEMANN, *Periodontology 2000*, **17** (1998) 7.
7. K. E. HEALY and P. DUCHEYNE, *Biomaterials* **13** (1992) 553.
8. D. M. BRUNETTE, in ''Surface characterization of Biomaterials'' (Elsevier Science Publisher B.V., Amsterdam, 1998) p. 203.
9. B. KASEMO and J. LAUSMAA, in ''The Bone-Biomaterials Interface'', edited by J. E. Davies (University of Toronto Press, Toronto, 1991) p. 19.
10. D. BUSER, R. K. SCHENK, S. STEINEMANN, J. P. FIORELLINI, C. H. FOX and H. STICH, *J. Biomed. Mater. Res.* **25** (1991) 889.
11. M. WONG, J. EULENBERGER, R. SCHENK and E. HUNZIKER, *ibid.* **29** (1995) 1567.
12. A. WENNERBERG, in ''On Surface Roughness and Implant Incorporation''. Dissertation, Göteborg University, Göteborg (1996) p. 65.
13. R. K. SCHENK and D. BUSER, *Periodontology 2000* **17** (1998) 22.
14. R. SOLAR, S. POLLAK and E. KOROSTOFF, *J. Biomed. Mater. Res.* **13** (1979) 217.
15. J. WOODMAN, J. JACOBS, J. GALANTE and R. URBAN, *J. Orthop. Res.* **1** (1984) 421.
16. M. WIELAND, C. SITTIG, M. TEXTOR, V. SCHENK, S.-W. HA, B. A. KELLER, E. WINTERMANTEL and N. D. SPENCER, *ECASIA97* (1997) p. 139.
17. A. ARYS, C. PHILIPPARD, N. DOUROV, Y. HE, Q. T. LE and J. J. PIREAUX, *J. Biomed. Res.* **43**(3) (1998) 300.
18. B. D. RATNER, in ''Surface Characterisation of Biomaterials'', (Elsevier Science Publishers B.V., Amsterdam, 1988) p. 13.
19. C. D. WAGNER, L. E. DAVIS, M. V. ZELLER, J. A. TAYLOR, R. M. RAYMOND and L. H. GALE, *Surf. Interf. Anal.* **3** (1981) 211.
20. R. N. S. SODHI, A. WENINGER, J. E. DAVIES and K. SREENIVAS, *J. Vac. Sci. Technol. A* **9**(3) (1991) 1329.

21. C. SITTIG, M. WIELAND, P.-H. VALLOTTO, M. TEXTOR and N. D. SPENCER, *J. Mater. Sci.: Mater. Med.* **10** (1998) 35.
22. C. SITTIG, in ''PhD thesis ETH Nr. 12657'', ETH Zürich, 1998.
23. J. F. MOLDER, W. F. STICKLE, P. E. SOBOL, K. D. BOMBEN and J. CHASTAIN, *Handbook of X-ray Photoelecyron Spectroscopy*, Perkin-Elmer Corporation, Physical Electronics Division, Minnesota (1992).
24. D. BRIGGS, A. BROWN and J. C. VICKERMAN, ''Handbook of Static Secondary Ion Mass Spectrometry'' (John Wiley & Sons, Chichester/New York/Brisbane/Toronto/Singapore, 1989) p. 50.

Received 30 March 2000
and accepted 29 June 2001